Freeze-out Conditions in Heavy Ion Collisions from QCD Thermodynamics

A. Bazavov,[1] H.-T. Ding,[1] P. Hegde,[1] O. Kaczmarek,[2] F. Karsch,[1,2] E. Laermann,[2] Swagato Mukherjee,[1] P. Petreczky,[1] C. Schmidt,[2] D. Smith,[2] W. Soeldner,[3] and M. Wagner[2]

[1] *Physics Department, Brookhaven National Laboratory, Upton, NY 11973, USA*
[2] *Fakultät für Physik, Universität Bielefeld, D-33615 Bielefeld, Germany*
[3] *Institut für Theoretische Physik, Universität Regensburg, D-93040 Regensburg, Germany*

(Dated: August 7, 2012)

We present a determination of chemical freeze-out conditions in heavy ion collisions based on ratios of cumulants of net electric charge fluctuations. These ratios can reliably be calculated in lattice QCD for a wide range of chemical potential values by using a next-to-leading order Taylor series expansion around the limit of vanishing baryon, electric charge and strangeness chemical potentials. From a computation of up to fourth order cumulants and charge correlations we first determine the strangeness and electric charge chemical potentials that characterize freeze-out conditions in a heavy ion collision and confirm that in the temperature range 150 MeV $\leq T \leq$ 170 MeV the hadron resonance gas model provides good approximations for these parameters that agree with QCD calculations on the (5-15)% level. We then show that a comparison of lattice QCD results for ratios of up to third order cumulants of electric charge fluctuations with experimental results allows to extract the freeze-out baryon chemical potential and the freeze-out temperature.

PACS numbers: 11.15.Ha, 12.38.Gc, 12.38Mh, 24.60-k

arXiv:1208.1220v1 [hep-lat] 6 Aug 2012

1) Introduction: A central goal of experiments at the Relativistic Heavy Ion Collider (RHIC) [1] is the exploration of the phase diagram of Quantum Chromodynamics (QCD) at non-zero temperature (T) and baryon chemical potential (μ_B). In particular, a systematic Beam Energy Scan (BES) is being performed at RHIC in order to search for evidence for or against the existence of the QCD critical point, a second order phase transition point, that has been postulated to exist at non-vanishing baryon chemical potential in the T-μ_B phase diagram of QCD [2, 3]. It would be the endpoint of a line of first order phase transitions which then would exist for larger μ_B. The measurement of fluctuations of conserved charges, e.g. net baryon number, electric charge and strangeness [4–6], plays a crucial role [7] in this search for critical behavior and the exploration of the QCD phase diagram in general.

Fluctuations of conserved charges generated in a heavy ion collision experiment may reflect thermal conditions at the time where the expanding medium, created in these collisions, cooled down and diluted sufficiently so that hadrons form again. It may be questioned whether the thermal medium at this time is in equilibrium and whether hadronization of all species takes place at the same time. However, statistical hadronization models, based on thermal hadron distributions given by the Hadron Resonance Gas (HRG) model, describe the hadronization process quite successfully [8]. Moreover, HRG model calculations of net baryon number fluctuations [9] describe well experimental data on net proton fluctuations [4]. This seems to suggest that at the time of chemical freeze-out the system can be described by thermodynamics characterized by a temperature T_f and a baryon chemical potential μ_B^f.

The measurement of conserved net charge fluctuations can provide a sensitive probe for critical behavior in hot and dense nuclear matter only when these fluctuations are generated at a point in the QCD phase diagram, characterized by $(T_f,\ \mu_B^f)$, that is close to the QCD transition line and eventually is also close to the elusive critical point. Lattice QCD calculations provide some information on the location of the QCD transition line in the T-μ_B plane at small values of the baryon chemical potential [10, 11]. The position of the freeze-out points in this phase diagram are usually determined by comparing experimental data on multiplicities of various hadron species with the HRG model calculation [8, 12]. In order to put these parameters on a firm basis and compare them with the QCD transition line it is desirable to extract the freeze-out parameters by comparing experimental data with a QCD calculation. This requires observables which are experimentally accessible and can also reliably be calculated in QCD. The fluctuations of conserved charges and their higher order cumulants form such a set of observables. While net baryon number fluctuations are experimentally accessible only through measurements of net proton number fluctuations [4], which may cause some difficulties [13, 14], electric charge fluctuations may be easier to analyze. We thus will focus on the latter. As an intermediate step one should also verify to what extent HRG model calculations and QCD calculations of freeze-out parameters yield consistent results when applied to the same set of thermal observables.

We present here a calculation of ratios of cumulants of net electric charge and net baryon number fluctuations that can be formed from the first three cumulants. They are related to mean (M_X) , variance (σ_X^2) and skewness (S_X) of the corresponding charge distributions,

$X = B,\ Q,\ S$ for baryon number, electric charge and strangeness, respectively. These ratios can be compared to HRG model calculations and will be used to extract the freeze-out temperature and baryon chemical potential from corresponding experimental measurements.

2) Strangeness and electric charge chemical potentials: In order to get access to T_f and μ_B^f we need to fix the electric charge (μ_Q) and strangeness (μ_S) chemical potentials that characterize a thermal system created in a heavy ion collision. They are determined by assuming that the thermal sub-volume, probed by measuring fluctuations in a certain rapidity and transverse momentum window, reflects the net strangeness content and electric charge to baryon number ratios of the incident nuclei,

$$M_S \equiv 0 \ , \ \ M_Q = r M_B \ , \tag{1}$$

where $M_X = (VT^3)^{-1}\partial \ln Z(\mu,T)/\partial\hat{\mu}_X$ is the expectation value of the density of net charge X, $\mu = (\mu_B,\ \mu_Q,\ \mu_S)$ summarizes the three charge chemical potentials and $\hat{\mu}_X \equiv \mu_X/T$. At any value of (T,μ_B) the chemical potentials (μ_Q,μ_S) that fulfill these constraints can be evaluated in QCD. We perform a Taylor expansion of the densities M_X in terms of the three chemical potentials and calculate the expansion coefficients of this series using the lattice regularization scheme. This involves the numerical calculation of generalized susceptibilities

$$\chi^{BQS}_{ijk,\mu} = \frac{1}{VT^3}\frac{\partial^{i+j+k}\ln Z(\mu,T)}{\partial\hat{\mu}_B^i\partial\hat{\mu}_Q^j\partial\hat{\mu}_S^k} \tag{2}$$

at $\mu = 0$. The calculation[1] of χ^{BQS}_{ijk} becomes computationally demanding at higher orders, but is done in lattice QCD with steadily increasing precision since many years [15]. In particular, recent calculations performed with the Highly Improved Staggered Quark (HISQ) action [16] and the stout action [17] provide continuum extrapolated results for all diagonal (χ_2^X) and off-diagonal (χ_{11}^{XY}) susceptibilities that are needed to determine $(\hat{\mu}_Q,\ \hat{\mu}_S)$ to leading order in $\hat{\mu}_B$.

Let us write the next-to-leading order (NLO) expansion of $\hat{\mu}_Q$ and $\hat{\mu}_S$ as

$$\hat{\mu}_Q = q_1\ \hat{\mu}_B + q_3\ \hat{\mu}_B^3\ ,\ \hat{\mu}_S = s_1\ \hat{\mu}_B + s_3\ \hat{\mu}_B^3\ . \tag{3}$$

Expanding the densities M_X up to third order in the chemical potentials we can fulfill the constraints specified in Eq. 1 at NLO. This provides four equations to determine the four parameters $(s_1,\ s_3,\ q_1,\ q_3)$. In leading order (LO) one obtains,

$$q_1 = \frac{r\left(\chi_2^B\chi_2^S - \chi_{11}^{BS}\chi_{11}^{BS}\right) - \left(\chi_{11}^{BQ}\chi_2^S - \chi_{11}^{BS}\chi_{11}^{QS}\right)}{\left(\chi_2^Q\chi_2^S - \chi_{11}^{QS}\chi_{11}^{QS}\right) - r\left(\chi_{11}^{BQ}\chi_2^S - \chi_{11}^{BS}\chi_{11}^{QS}\right)}\ ,$$

$$s_1 = -\frac{\chi_{11}^{BS}}{\chi_2^S} - \frac{\chi_{11}^{QS}}{\chi_2^S}\ q_1\ . \tag{4}$$

The NLO expressions are lengthy but can be derived easily [20]. We evaluated the leading order expressions in the temperature interval 150 MeV $\leq T \leq$ 250 MeV for three different values of the lattice cut-off (a) corresponding to lattices with temporal extent $N_\tau \equiv 1/aT = 6,\ 8$ and 12. All calculations have been performed within an $\mathcal{O}(a^2)$ improved gauge and staggered fermion (HISQ) discretization scheme [19] for (2+1)-flavor QCD. The strange quark mass has been tuned to its physical value and the light to strange quark mass ratio is fixed to $m_l/m_s = 1/20$, which leads to a lightest Goldstone pion mass of about 160 MeV. In the calculation of leading order results for $\hat{\mu}_S$ and $\hat{\mu}_Q$ we make use of data obtained by the HotQCD collaboration [16]. On the $24^3\times 6$, and $32^3\times 8$ lattices we extended these calculations in the temperature interval 150 MeV $\leq T \leq$ 175 MeV to 30,000 molecular dynamics time units, saving configurations after every 10^{th}, and by increasing the number of random vectors used to evaluate the susceptibilities to 1500 per gauge field configuration.

We will in the following restrict our discussion to the case, $r = 0.4$, which approximates well the situation met in Au-Au as well as Pb-Pb collisions. The leading order expansion coefficients for $\hat{\mu}_Q$ and $\hat{\mu}_S$ are shown in the top panels of Fig. 1 left and middle. Using spline interpolations of numerical results obtained for three different lattice sizes, we performed extrapolations to the continuum limit using an ansatz linear in $1/N_\tau^2$. We have checked that no statistically significant differences occur by including an additional $1/N_\tau^4$ correction. The resulting extrapolations are shown as bands in these panels.

In order to check the importance of NLO corrections we have calculated s_3 and q_3 on lattices with temporal extent $N_\tau = 6$ and 8. The results, expressed in units of the leading order terms, are also shown in Fig. 1. It is obvious from this figure that NLO corrections indeed are small. They are negligible in the high temperature region and are below 10% in the temperature interval relevant for the analysis of freeze-out conditions, i.e., $T \simeq (160 \pm 10)$ MeV. In fact, in this temperature range the leading order lattice QCD results deviate from HRG model calculations expanded to the same order by less than 15%. The next to leading order corrections start to become smaller than the HRG model values for $T \gtrsim 160$ MeV. This further reduces the importance of NLO corrections. In this respect we note that in the HRG model the NLO expansion reproduces the full HRG result for $\hat{\mu}_Q$ and $\hat{\mu}_S$ to better than 1.0% for all values of $\mu_B/T \leq 1.3$. Altogether, we thus expect that the NLO-truncated QCD expansion is a good approximation to the complete QCD results for $\hat{\mu}_Q$ and $\hat{\mu}_S$ for $\mu_B \leq 200$ MeV.

In order to address further systematic errors we note that in a lattice QCD study as ours which utilizes the staggered discretization scheme, the biggest cut-off ef-

[1] In the following subscripts and the corresponding superscripts are suppressed in cases where the former is zero; furthermore the abbreviation $\chi^{BQS}_{ijk} = \chi^{BQS}_{ijk,\mu=0}$ is used.

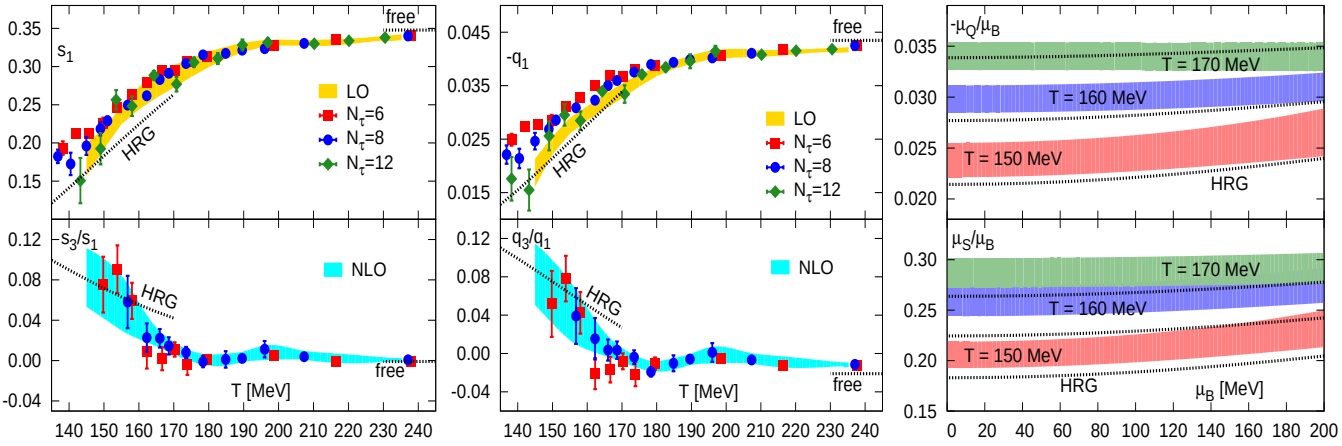

FIG. 1. The leading and next-to-leading order expansion coefficients of the strangeness (left) and the negative of the electric charge chemical potentials (middle) versus temperature for $r = 0.4$. For s_1 and q_1 the LO-bands show results for the continuum extrapolation. For s_3 and q_3 we give an estimate for continuum results (NLO bands) based on spline interpolations of the $N_\tau = 8$ data. Dashed lines at low temperature are from the HRG model and at high temperature from a massless, 3-flavor quark gas. The right hand panel shows NLO results for μ_S/μ_B and μ_Q/μ_B as function of μ_B for three values of the temperature.

fects at non-vanishing lattice spacing are generally due to so-called taste violations. These give rise to a distorted hadron spectrum but mainly influence the pion sector [16]. Correspondingly the electric charge susceptibilities will be the ones most sensitive to discretization effects while the baryon and strangeness sectors are largely unaffected. At leading order these discretization effects have been eliminated by taking the continuum limit. At NLO taste violation effects show up in the electric charge sector, Fig.1(middle). However, as the corrections themselves are already small, we expect their influence to be small. Furthermore, the taste violations can be modelled within the HRG model by replacing the pion mass with the average, root mean-square pion mass [16] of our lattice calculations. Results obtained with this modified spectrum suggest that taste violation effects are indeed negligible in the NLO calculation of the strangeness chemical potential and lead to at most 5% systematic errors in $\hat{\mu}_Q$ for $\mu_B \leq 200$ MeV.

Additional systematic errors arise from the fact that we perform calculations with degenerate light quark masses $m_u = m_d$, as is usually done in current lattice QCD calculations. As a consequence not all susceptibilities χ^{BQS}_{ijk} are independent; actually there are two constraints in leading order ($\chi^B_2 = 2\chi^{BQ}_{11} - \chi^{BS}_{11}$, $\chi^S_2 = 2\chi^{QS}_{11} - \chi^{BS}_{11}$) and six constraints in next to leading order [20]. These constraints of course, do not hold in the HRG model and may be considered as an additional source for the distortion of the hadron spectrum. Imposing these constraints by hand in the HRG model calculations we find that q_1 and q_3 can change by up to 3% while modifications of s_1 and s_3 are below the 1% level. This suggests that even after extrapolating to the continuum limit, the current lattice QCD calculations of μ_Q/μ_B do have an inherent systematic error of about 3%.

Our results for the strangeness and electric charge chemical potentials at NLO as function of μ_B and T are shown in Fig. 1(right). While μ_S/μ_B varies between 0.2 and 0.3 in the interval 150 MeV $\leq T \leq$ 170 MeV, the absolute value of μ_Q/μ_B is an order of magnitude smaller. Both ratios are almost constant for $\mu_B \leq 200$ MeV, which is consistent with HRG model calculations.

3) Ratios of cumulants of net charge fluctuations: We now are prepared to evaluate cumulants of net charge fluctuations at as function of T and μ_B at non-vanishing values for μ_S and μ_Q that obey the constraints appropriate for thermal conditions met in a heavy ion collision, i.e., Eq. 1. Of particular interest are ratios of cumulants, $R^X_{nm} = \chi^X_{n,\mu}/\chi^X_{m,\mu}$, which to a large extent eliminate the dependence of cumulants on the freeze-out volume. Ratios with $n + m$ even are non-zero for $\mu = 0$, while the odd-even ratios are in leading order proportional $\hat{\mu}_B$ and thus vanish for $\mu = 0$. Ratios with $n + m$ even or odd thus provide complementary information on T_f and μ^f_B. We will concentrate here on the simplest such ratios,

$$R^X_{12} \equiv \frac{M_X}{\sigma^2_X} = \hat{\mu}_B \left(R^{X,1}_{12} + R^{X,3}_{12}\, \hat{\mu}^2_B + \mathcal{O}(\hat{\mu}^4_B) \right) , \quad (5)$$

$$R^X_{31} \equiv \frac{S_X \sigma^3_X}{M_X} = R^{X,0}_{31} + R^{X,2}_{31}\, \hat{\mu}^2_B + \mathcal{O}(\hat{\mu}^4_B) , \quad (6)$$

with $X = B,\ Q$. These ratios can be calculated in QCD as well as in the HRG model [7], and eventually can be compared to experimental data in order to determine T_f and μ^f_B. We evaluated them up to $\mathcal{O}(\hat{\mu}^3_B)$ in a Taylor expansion for R^X_{12} and to leading order for R^X_{31}.

Let us first discuss the odd-even ratios R^X_{12}. Using $\chi^{XX}_{11} \equiv \chi^X_2$ the LO coefficients can be written as

$$R^{X,1}_{12} = \frac{\chi^{BX}_{11}}{\chi^X_2} + q_1 \frac{\chi^{XQ}_{11}}{\chi^X_2} + s_1 \frac{\chi^{XS}_{11}}{\chi^X_2} , \quad (7)$$

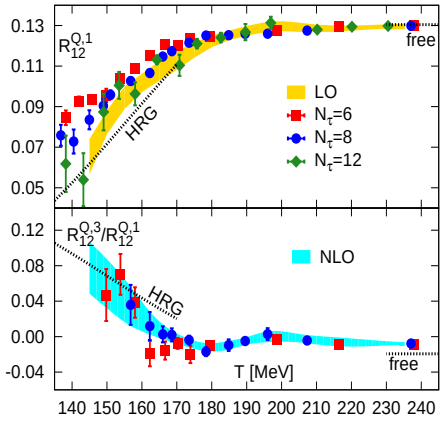

FIG. 2. The leading (top) and next-to-leading (bottom) order expansion coefficients of the ratio of first to second order cumulants of net electric charge fluctuations versus temperature for $r = 0.4$. The bands and lines are as in Fig. 1(left).

with $X = B,\ Q$. They have been evaluated on lattices with temporal extent $N_\tau = 6,\ 8$ and 12 and have been extrapolated to the continuum limit in the same way as for q_1 and s_1. The LO ratio $R_{12}^{Q,1}$, evaluated for three different values of the lattice cut-off (data points) and the resulting continuum extrapolation (LO band) are shown in Fig. 2(top). In Fig. 2(bottom) we show the NLO corrections which have been evaluated on lattices with temporal extent $N_\tau = 6$ and 8. The NLO corrections to the ratio of electric charge cumulants are below 10%, which makes the leading order result a good approximation for a large range of $\hat{\mu}_B$. Systematic errors arising from the truncation of the Taylor series for R_{12}^Q at next-to-leading order may again be estimated by comparing the full result in the HRG model calculation with the corresponding truncated results. Here we find for $T = (160 \pm 10)$ MeV and $\mu_B/T \leq 1.3$ that the difference is less than 1.0%. Moreover, we estimated that taste violation effects in the NLO calculation lead to systematic errors that are at most 5% and thus will be negligible in R_{12}^Q. Taylor series truncated at NLO are thus expected to give a good approximation to the full result for a wide range of baryon chemical potentials. Similar results hold for the ratio R_{12}^B, although NLO corrections are larger in this case.

4.) Determination of freeze-out baryon chemical potential and temperature: Obviously the ratio R_{12}^Q shows a strong sensitivity on μ_B but varies little with T for $T \simeq (160 \pm 10)$ MeV. We show this ratio, evaluated in this temperature interval in a NLO Taylor expansion, in Fig. 3(left) as function of $\hat{\mu}_B$. For the determination of (T_f, μ_B^f) a second, complimentary information is needed. To this end we use the ratio R_{31}^Q, which is strongly dependent on T but receives corrections only at $\mathcal{O}(\hat{\mu}_B^2)$. The leading order result for this ratio is shown in Fig. 3(middle). Apparently this ratio shows a characteristic temperature dependence for $T \gtrsim 155$ MeV that is quite different from that of HRG model calculations. The NLO correction to this ratio vanishes in the high temperature limit and at low T the HRG model also suggests small corrections. In fact, in the HRG model the LO contributions to R_{31}^Q differ by less than 2% from the exact results on the freeze-out curve for $\mu_B \leq 200$ MeV. In the transition region a preliminary 6^{th} order calculation at $T = 162$ MeV [20] suggests that the μ_B^2 correction in units of the LO term is $-0.03(10)$. Based on these estimates in the three T regions we expect the NLO corrections to be of the order of 10% for the whole temperature range. In Fig. 3(middle) we show the spline interpolation for the $N_\tau = 8$ data as a band and added on top of this a band that estimates the effect of a 10% contribution of the NLO correction. The ratio R_{31}^Q thus seems to be well suited for a determination of the freeze-out temperature.

We now are in the position to extract μ_B^f and T_f from R_{12}^Q and R_{31}^Q which eventually will be measured in the BES at RHIC. A large value for R_{31}^Q, i.e. $R_{31}^Q \simeq 2$ would suggest a low freeze-out temperature $T \lesssim 155$ MeV, while a value $R_{31}^Q \simeq 1$ would suggest a large freeze-out temperature, $T \sim 170$ MeV. A value of $R_{31}^Q \simeq 1.5$ would correspond to $T \sim 160$ MeV.

A measurement of R_{31}^Q thus suffices to determine the freeze-out temperature. In the HRG model parametrization of the freeze-out curve [12] the favorite value for T_f in the beam energy range 200 GeV $\geq \sqrt{s_{NN}} \geq 39$ GeV indeed varies by less than 2 MeV and is about 165 MeV. At this temperature the values for R_{31}^Q calculated in the HRG model and in QCD differ quite a bit, as is obvious from Fig. 3. While $R_{31}^Q \simeq 2$ in the HRG model, one finds $R_{31}^Q \simeq 1.2$ in QCD at $T = 165$ MeV. Values close to the HRG value are compatible with QCD calculations only for $T \lesssim 157$ MeV. We thus expect to either find freeze-out temperatures that are about 5% below HRG model results or values for R_{31}^Q that are significantly smaller than the HRG value. A measurement of this cumulant ratio at RHIC thus will allow to determine T_f and probe the consistency with HRG model predictions.

For any of these temperature values a comparison of an experimental value for R_{12}^Q with Fig. 3(left) will allow to determine μ_B^f. To be specific let us discuss the results obtained at $T = 160$ MeV. Here we find

$$R_{12}^Q(T = 160 \text{ MeV}) = 0.102(5)\hat{\mu}_B + 0.002(1)\hat{\mu}_B^3 \,. \quad (8)$$

For a value of the freeze-out temperature close to $T = 160$ MeV we thus expect to find $\mu_B^f = (20-30)$ MeV, if R_{12}^Q lies in the range $0.012-0.020$, $\mu_B^f = (50-70)$ MeV for $0.032 \leq R_{12}^Q \leq 0.045$ and $\mu_B^f = (80-120)$ MeV for $0.05 \leq R_{12}^Q \leq 0.08$. These parameter ranges are expected [1, 12, 18] to cover the regions relevant for RHIC beam energies $\sqrt{s_{NN}} = 200$ GeV, 62.4 GeV and 39 GeV, respectively. As is evident from Fig. 3(left) the values for μ_B^f will shift to smaller (larger) values when T_f turns out to be larger (smaller) than 160 MeV. A more refined

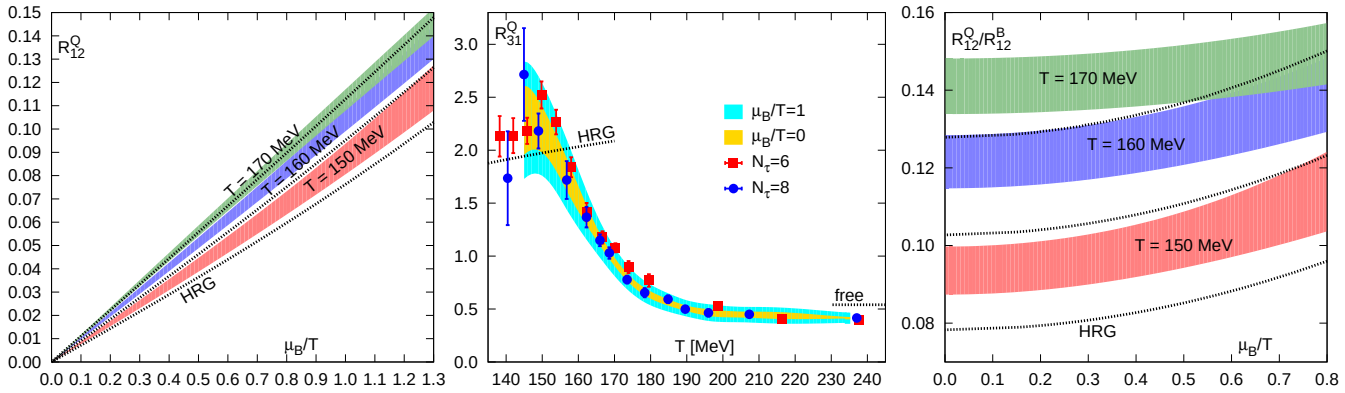

FIG. 3. The ratios R^Q_{12} versus μ_B/T (left) for three values of the temperature and R^Q_{31} versus temperature for $\mu_B = 0$ (middle). The wider band on the data set for $N_\tau = 8$ (middle) shows an estimate of the magnitude of NLO corrections. The right hand panel shows the NLO result for the ratio of ratios of net electric charge and baryon number fluctuations, respectively.

analysis of (T_f, μ^f_B) will become possible, once the ratios R^Q_{12} and R^Q_{31} have been measured experimentally.

5) Conclusions: We have shown that the first three cumulants of net electric charge fluctuations are well suited for a determination of freeze-out parameters in a heavy ion collision. Although the ratios R^Q_{12} and R^Q_{31} are sufficient to determine T_f and mu^f_B, it will clearly be advantageous to have several ratios, including cumulants of net baryon number fluctuations, at hand that will allow to probe the consistency of an equilibrium thermodynamic description of cumulant ratios at the time of freeze-out. In particular the ratio of ratios $R^Q_{12}/R^B_{12} = r\chi^B_{2,\mu}/\chi^Q_{2,\mu}$ is also well determined in (lattice) QCD calculations [16]. In Fig. 3(right) we show the NLO result for this ratio of ratios in the temperature range $T = (160 \pm 10)$ MeV. Its measurement will, on the one hand, allow to probe our basic assumptions on constraining the electric charge and strangeness chemical potentials and, on the other hand, constrain possible differences in cumulant ratios of net proton and net baryon number fluctuations. Once the ratios of lower order cumulants have been used to fix the freeze-out parameters, the calculation of higher order cumulants is parameter free and provides unique observables for the discussion of possible signatures for critical behavior along the freeze-out line.

Acknowledgements: We thank P. Bialas, T. Luthe and L. Wresch for discussions and help with the software development for the Bielefeld GPU cluster. Numerical calculations have also been performed on the USQCD GPU-clusters at JLab and NYBlue at the NYCCS. This work has been supported in part by contract DE-AC02-98CH10886 with the U.S. Department of Energy, the Bundesministerium für Bildung und Forschung under grant 06BI9001, the Gesellschaft für Schwerionenforschung under grant BILAER, the Deutsche Forschungsgemeinschaft under grant GRK881, and the EU Integrated Infrastructure Initiative Hadron-Physics2.

[1] B. Mohanty [STAR Collaboration], J. Phys. G **38**, 124023 (2011).
[2] M. Asakawa, K. Yazaki, Nucl. Phys. A **504**, 668 (1989).
[3] J. Berges, K. Rajagopal, Nucl. Phys. B **538**, 215 (1999); A. M. Halasz et al., Phys. Rev. D **58**, 096007 (1998).
[4] M. M. Aggarwal *et al.* [STAR Collaboration], Phys. Rev. Lett. **105**, 022302 (2010).
[5] A. Adare *et al.* [PHENIX Collaboration], Phys. Rev. C **78**, 044902 (2008).
[6] B. Abelev *et al.*, [ALICE Collaboration], arXiv:1207.6068 [nucl-ex].
[7] S. Ejiri, F. Karsch, K. Redlich, Phys. Lett. B **633**, 275 (2006).
[8] P. Braun-Munzinger, K. Redlich, J. Stachel, In *Hwa, R.C. (ed.) et al.: Quark gluon plasma* 491-599.
[9] F. Karsch and K. Redlich, Phys. Lett. B **695**, 136 (2011); P. Braun-Munzinger *et al.*, Phys. Rev. C **84**, 064911 (2011).
[10] O. Kaczmarek *et al.*, Phys. Rev. **D83**, 014504 (2011).
[11] G. Endrodi *et al.*, JHEP **1104**, 001 (2011).
[12] J. Cleymans *et al.*, Phys. Rev. C **73**, 034905 (2006).
[13] M. Kitazawa, M. Asakawa, Phys. Rev. C **85**, 021901 (2012).
[14] A. Bzdak, V. Koch, V. Skokov, arXiv:1203.4529 [hep-ph].
[15] R. V. Gavai, S. Gupta, Phys. Rev. D **68**, 034506 (2003); C. R. Allton et al., Phys. Rev. D **71**, 054508 (2005); M. Cheng et al., Phys. Rev. D **79**, 074505 (2009).
[16] A. Bazavov *et al.* [HotQCD Collaboration], arXiv:1203.0784 [hep-lat]. and Phys. Rev. D **85**, 054503 (2012).
[17] S. Borsanyi *et al.*, JHEP **1201**, 138 (2012).
[18] B. I. Abelev *et al.* [STAR Collaboration], Phys. Rev. C **79**, 034909 (2009).
[19] E. Follana *et al.* [HPQCD and UKQCD Collaborations], Phys. Rev. D **75**, 054502 (2007).
[20] Bielefeld-BNL Collaboration, in preparation.